Building and Environment 233 (2023) 110104

Contents lists available at ScienceDirect

Building and Environment

journal homepage: www.elsevier.com/locate/buildenv

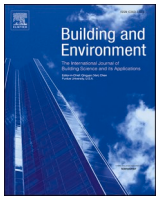

Future weather generator for building performance research: An open-source morphing tool and an application

Eugénio Rodrigues [a,*], Marco S. Fernandes [a], David Carvalho [b]

[a] Univ of Coimbra, ADAI, Department of Mechanical Engineering, Rua Luís Reis Santos, Pólo II, 3030-788, Coimbra, Portugal
[b] CESAM, Physics Department, University of Aveiro, 3810-193, Aveiro, Portugal

ARTICLE INFO

Keywords:
Future weather
Weather morphing
Climate change
Building
Energy performance

ABSTRACT

Mathematical morphing of historical weather data to match the projected climate change scenario is a commonly used method to generate future weather files for building energy simulation. It is known for preserving the local weather characteristics, which is particularly important when designing or analyzing high-performance buildings. Researchers may use one of the available morphing tools. Unfortunately, current tools use future climate data from outdated climate models with lesser accuracy, coarser spatial resolution, and fewer climate scenarios than recent models. In addition, these tools are closed, preventing others from adding corrections, updating, and developing them further. This paper presents an open-source, cross-platform, and state-of-the-art morphing tool that generates future hourly weather data for the whole building performance simulation. The novel tool is applied to a real-case office building in Coimbra, Portugal. In the SSP5-8.5 scenario, simulations show thermal energy needs and electricity use will reduce by 60% in 2050 and 77% in 2080 for heating and will increase by 67% in 2050 and 121% in 2080 for cooling. As a result, the building's global electricity consumption will increase by 24% in 2050 and by 53% in 2080. The study is extended to other locations in Europe, concluding that the total HVAC energy needs will remain constant or even decrease in heating-dominated climates, mainly due to the significant drop in the heating demand in the future.

1. Introduction

The morphing method transforms mathematically present-day weather to match projected variables of a climate change scenario from numerical models that represent the physical processes in the atmosphere, ocean, cryosphere, and land surface (general circulation model—GCM; regional climate model—RCM) [1]. To guarantee the method's accuracy, the period of the present-day records and the baseline of the changes must match. Since it transforms present-day records, morphing preserves the local climate characteristics and assumes that today's weather patterns will be the same in the future [2]. This aspect of the morphing method is important as it reduces the risk of creating ill-designed buildings for a specific location, thus undermining a nation's capability to meet its carbon neutrality targets [3].

The morphing method is also a fast and easy-to-use procedure with minimal computing resources—building performance researchers tend to select the simplest-to-use weather generator [4], thus contributing to being the most used approach [5]. In addition, morphing is essentially a delta method [6] as it only requires future changes of the projected variables to transform historical weather records, thus avoiding the need to adjust the simulated data of the reference period to the historical records (bias correction). These characteristics make morphing an ideal method, resulting in bearable size tools. These advantages contrast with the other weather generation procedures, which require more computing resources, a larger amount of data for the same spatial and temporal resolution, and pos-processing for correcting the climate model bias. The latter procedures require computing multi-year hourly climate data and downscaling it when the resolution is too coarse, assuming that large-scale meteorology and geographic features influence local weather and climate [2].

Morphing presents some shortfalls, such as (i) disregarding the increase in severity of extreme weather and its frequency, (ii) overestimating extreme data as it approaches maximum and minimum temperatures independently from the mean value [7], (iii) not guaranteeing the consistency of the relationship between some of the climate variables [8], and (iv) constraining the applicability to weather records with similar baseline periods [5]. However, morphing is suitable if the purpose is to estimate the building energy performance over a long

* Corresponding author.
E-mail address: erodrigues@uc.pt (E. Rodrigues).

https://doi.org/10.1016/j.buildenv.2023.110104
Received 24 October 2022; Received in revised form 18 January 2023; Accepted 13 February 2023
Available online 14 February 2023

period [6]. For a detailed comparison with competing methods, see Refs. [2,5,9,10].

Currently, there are three weather morphing tools available to researchers: the WeatherShift [11], 'Weather Morph' [12], and the CCWorldWeatherGen [8]—the latter being the most widely used by researchers studying buildings' energy performance [13] despite not being maintained since 2017. Table 1 lists the main characteristics of each tool, such as the used climate data, IPCC report, scenarios, and timeframes. The main characteristics of these tools are the coarse spatial resolution, outdated climate model data, a small number of climate scenarios, and an old baseline period.

Nonetheless, researchers still use these tools. For example, Lapisa et al. [14] optimized a commercial building envelope design to minimize energy consumption and thermal discomfort under climate change in France. The future climate was morphed using CCWorldWeatherGen for scenario A2 in the 2070–2099 timeframe. The results demonstrated that summer thermal discomfort could be reduced, and an active cooling system may not be needed for some locations. Another example of using this tool is provided by Cirrincione et al. [15], who studied the benefits of green roofs in the A2 scenario. The authors found that green roofs can contribute up to 50% and 15% energy reduction during the cooling season in Luxembourg and Italy, respectively. In order to analyze different ventilation strategies, Bamdad et al. [16] morphed historical weather data from several locations in Australia using 'Weather Morph.' Results showed energy-saving potential of mixed-mode ventilation with or without ceiling fans will maintain or decrease for scenarios A1F1 and B2 in the 2070–2099 timeframe, depending on the climate zone. Finally, Baba et al. [17] used WeatherShift to analyze the overheating of high-energy-efficient buildings in 2026–2045 and 2081–2100 timeframes for RCP 4.5 and RCP 8.5 scenarios in Canada. The authors found that adequate ventilation is needed to prevent overheating.

Unfortunately, these tools share one or more disadvantages or issues [5] that hinder the tools' accuracy, reliability, and, nowadays, scientific significance. Table 2 lists all the advantages and weaknesses of each tool. The critical aspects are.

- The tool may use data from 21-year-old numerical models with a coarse spatial resolution (or limited to a predetermined number of cities), a small number and outdated scenarios, and already outdated timeframes.
- The tool may have monthly changes obtained from two unmatching world grids.
- The tool may have an old baseline period that prevents the morphing of recent weather records.
- The numerical model used in the tool might not provide all the monthly changes needed to morph current weather for some of the climate scenarios.
- When an ensemble of numerical models is used, these are unspecified by the developers.
- Weather observation flags are set missing or do not morph all needed variables in dynamic simulation.

Besides the mentioned aspects, CCWorldWeatherGen presents other issues (also applicable to 'Weather Morph'), such as (i) the baseline limits the morphing to historical records between 1961 and 1990, (ii) the climate variables are from two different spatial grids, and (iii) the final scenario results from averaging the mean changes of three scenarios. In addition, not all variables are available for the three scenarios.

In the case of 'Weather Morph,' it has the advantage of being self-contained and straightforward. However, it is not explained how A1F1, B1, and B2 scenarios are morphed, considering that the IPCC's website does not have all the variables needed to carry out the procedure [18].

Relatively to WeatherShift, the tool is a web service with very little information available; therefore, we do not know precisely how the morphing procedure is carried out. Nonetheless, according to the tool's website and a single conference communication [19], WeatherShift implements the simulation results from the climate models used in the 2014 IPCC's 5th Assessment Report. Instead of using a world grid as CCWorldWeatherGen, the tool uses an ensemble of numerical models (unspecified) to morph weather from 259 cities. The tool determines the monthly changes based on the Finkelstein-Schafer statistic, which is used to build a typical meteorological year (TMY) from a multi-year

Table 1
Climate model features in the morphing tools.

Tool	Data	IPCC Report	Scenarios	Timeframes
CCWorldWeatherGen	HadCM3, world grid, CMIP2 Resolution of 2.5° latitude and 3.75° longitude 417 km × 278 km, reduces to 295 km × 278 km at 45° N/S Average of the four nearest points Mean changes	2001, 3rd	A2	Baseline 1961–1990 2020 (2010–2039) 2050 (2040–2069) 2080 (2070–2099)
Weather Morph (An online version of CCWorldWeatherGen)	HadCM3, world grid, CMIP2 Resolution of 2.5° latitude and 3.75° longitude 417 km × 278 km, reduces to 295 km × 278 km at 45° N/S Average of the four nearest points Mean changes	2001, 3rd	A1F1, B1, A2, B2	Baseline 1961–1990 2020 (2010–2039) 2050 (2040–2069) 2080 (2070–2099)
WeatherShift	Ensemble of Models, 259 cities, CMIP5 Unknown resolution of the models Bilinear interpolation of the four nearest points Finkelstein-Schafer statistic of air temperature for 10%, 25%, 50%, 75%, and 90% percentiles	2014, 5th	RCP-4.5, RCP-8.5	Baseline 1976–2005 2035 (2026–2045) 2065 (2056–2075) 2090 (2081–2100)

Table 2
Advantages and disadvantages of the currently available morphing tools.

Tool	Advantages and features	Disadvantages, issues, and limitations
CCWorldWeatherGen	• Free to use • Implementation is described in articles and the reference manual • Morphs weather data from any location in the world	• Outdated numerical model • The baseline prevents the use of recent meteorological records • It has two world grids with a large resolution that do not match • Only the A2 scenario is available • Averages scenarios A2a, A2b, and A2c to obtain A2 • Not all climate variables are available for the three timeframes • One of the 'future' timeframes is already outdated • Calculates the four points in the grid incorrectly for the wind variable • No interpolation (averages the four nearest grid points) • Month transition smoothness is hardcoded • It has an issue with atmospheric pressure at sea level unit conversion • Sets to missing the 'Present Weather Observation' and 'Present Weather Code' variables (prevents wet surfaces and snow reflection calculations) • Lacks the generation of the warmest and coldest years • It does not calculate the typical/extreme periods • Closed implementation (not reproducible) • Dependent on third-party commercial software • Limited to Windows operating systems • It is not a self-contained tool; it requires the user to download the climate data separately • No longer maintained (since 2017)
Weather Morph[a]	• Self-contained tool and straightforward to use • It has additional future scenarios	• Not all climate variables are available for all scenarios on the IPCC website for HadCM3 (no description of how this was overcome is given)
WeatherShift	• Allows other percentiles besides the 50% percentile (sorted according to a cumulative distribution function of the mean daily temperature), thus generating warmer and colder years for each timeframe • It uses a bilinear interpolation of the four nearest points • Presently supported and maintained (non-collaboratively)	• Only morphs data for 259 cities (no world grid) • Outdated numerical models • Baseline does not accept the most recent meteorological data • No detailed documentation on the implementation of the tool or the numerical models used; therefore, an accurate assessment of the tool is not possible • Closed implementation (not reproducible) • Not free to use

[a] As implementation follows CCWorldWeatherGen, only relevant differences are pointed out.

database. Briefly, the TMY procedure selects each month by comparing each month's long-term cumulative distribution function with the one of each year for selected variables—WeatherShift only uses air temperature. The month with a lower weighted Finkelstein-Schafer value is selected. However, the remaining month variables are not part of the calculation and may vary significantly depending on the year of that month—this variation also occurs for selected variables with low weights, showing lower agreement with long-term data [20]. Therefore, the monthly changes based on the difference between the climate model's TMYs simulated past and future periods may disrupt the variables' relationship consistency in the to-be-morphed TMY data. The authors of WeatherShift claim a consistent relationship between the variables [19], but no evidence is given. Lastly, WeatherShift uses a bilinear interpolation of the four nearest points to spatially downscale to the EPW location.

The tools also present other drawbacks that are, on some level, related to the issues mentioned above, the most noticeable being their code closedness that prevent corrections and improvements by the scientific community. Another drawback is being paid service or dependent on commercial third-party software. For example, CCWorldWeatherGen requires a commercial third-party spreadsheet to run, and WeatherShift is a web-based commercial service. 'Weather Morph' is also a web tool, but it is an online implementation of the CCWorldWeatherGen [21]. Although CCWorldWeatherGen and 'Weather Morph' are free to use, these are closed implementations without an accessible source code.

Alternatively, researchers may develop their morphing procedure, but it is cumbersome and time-consuming for those who aspire to study the climate change impacts on the built environment. For instance, Zou et al. [22] implemented a morphing procedure using the GISS-E2-R model (CMIP5) to transform present-day records ranging between 1985 and 2004 into RCP 4.5 and RCP 8.5 scenarios for all future years between 2020 and 2099. The procedure was used to analyze the impact of climate change on a reference building in several locations in China. A sensitivity analysis showed that the most efficient passive design strategies would be the construction type of walls and roofs, windows' solar heat gain coefficients, and the amount of window area. Silva et al. [23] implemented a morphing procedure using data from an ensemble of 21 climate models (CMIP5) to predict RCP 4.5 for the 2040–2049 timeframe. Present-day records, ranging between 2010 and 2019, were morphed to predict the impact of cooling measures on the building stock in Switzerland. The authors concluded that window shading and night ventilation are the major contributors to reduce by up to 84% in cooling demand. Bamdad et al. [24] used morphed data available from the Swiss National Centre for Climate Services website [25] that resulted from the combined use of ACCESS1.0, CESM1-CAM5, CNRM-CM5, GFDL-ESM2M, HadGEM2-CC, CanESM2, MIROC5, and NorESM1-M models (CMIP5), which depended on the location of each city in Australia. The morphed data was created for future years according to RCP 2.6 and RCP 8.5 scenarios from a baseline ranging from 1990 to 2015. The authors analyzed the benefits of natural ventilation and demonstrated that the total climatic potential for natural ventilation varied between −14.3% and +27%, depending on the current climate zone. Lastly, Shi et al. [26] implemented a morphing procedure with the CMCC-CM2-SR5 model (CMIP6) to morph present-day weather data, ranging between 1971 and 2000, into 2021–2050 timeframe for the Shared Socioeconomic Pathways (SSP) SSP1-2.6, SSP2-4.5, SSP3-7.0, and SSP5-8.5. The morphing procedure helped researchers simulate green roofs and natural night ventilation strategies to reduce the impact of global warming in China, which resulted in up to 18.7% improvement in energy savings. Again, as for the available tools, none of these studies share the source code of the morphing procedure, and only one study uses the latest climate model data from CMIP6 experiments.

This closedness may limit research. In fact, the scientific community argues for the release of source codes for reproducibility reasons [27]. Researchers argue that even if they describe the tool in detail, errors, ambiguities, and divergencies in hardware and software configurations may compromise reproducibility [27]. In addition, other benefits of releasing the code encompass an increase in the quality of the code, reduced errors, and greater efficiency due to code reuse and sharing [28]. Researchers may also benefit from customizing scientific software, obtaining economic savings since commercial-based technologies have higher research costs [29]. Finally, although some argue that transparency may lead others to develop competing tools or tackle a research problem first, others state that open-source code promotes collaboration [30]. Such collaboration fosters transdisciplinary research dialogs and creates a community to maintain and carry out further software developments [30]. Therefore, an ideal scientific tool should be free (without costs or legal restrictions), open (code available to the public), cross-platform (runnable on any platform), extendable (anyone can add or suggest new features), customizable (anyone can change it to fit specific research needs), and maintainable (especially by the scientific community).

The mentioned characteristics are not fully satisfied in today's tools for generating future weather using morphing. Ultimately, this situation hampers the capability of the scientific community to fight climate change and substantially reduces the speed of scientific discovery. Global warming challenges the built environment as boundary conditions shift toward a warmer and erratic climate [31]. In order to create low-energy buildings, professionals need adequate design strategies and guidelines [32], which require researchers to study how buildings will behave in a specific location using synthetically-generated future hourly weather data [13].

This paper presents a new morphing tool for building performance researchers with the latest state-of-the-art climate numerical data, a finer grid resolution, a better spatial interpolation method, a larger number of morphing variables, and a greater number of up-to-date climate change scenarios and timeframes (including the warmest and coldest years, besides the typical year). This tool is open, cross-platform, and free to use, allowing researchers to customize and extend it to meet their research needs, such as by adding other climate models and variables. In addition, this paper fills the need for a state-of-the-art weather morphing tool and, ultimately, promotes scientific discovery and research reproducibility. Lastly, the tool is demonstrated in a real-case office building in Coimbra, Portugal, and the results are compared with other European climate regions.

2. Materials and methods

The morphing procedure requires the user to provide an EnergyPlus Weather (EPW) file. The EPW file contains the weather station location, design conditions, typical/extreme periods, ground temperatures, holiday/daylight savings, run period, comments, optional data periods, and the actual weather data [33]. Each weather data entry consists of 34 numeric variables and one string with data source and uncertainty flags (Table 3 lists the variables). The EPW files may originate from different sources and be derived from different methodologies. Several websites allow downloading free EPW files, such as the EnergyPlus [34] and the Climate.OneBuilding.Org websites [35].

The tool features the monthly changes for EC-Earth3 [36] used in the CMIP6 project [37], which served as a basis for the 6th IPCC Assessment Report, published in 2022. EC-Earth3 was chosen for its high accuracy—*i.e.*, statistically indistinguishable. For example, the 20-year mean differences between the model performance against the reanalysis product ERA40 were 1.2% for the air temperature at 2 m, 0.7% for mean sea level pressure, 0.8% for net thermal radiation, and 0.7% for specific humidity [36].

When compared to MPI-ESM1-2-HR, MRI-ESM2-0, and NorESM2-MM models, which are the only CMIP6 GCMs that have available data for all variables for the four SSPs here considered (SSP1-2.6, SSP2-4.5, SSP3-7.0, and SSP5-8.5), EC-Earth3 presents finer spatial resolution with higher grid points, consistent high overlap percentage (OP), and low median differences (Δ medians) for minimum, maximum, and mean daily air temperatures (see Table 4). As OP captures the similarity between the probability density functions of the modeled and reference (ERA5) variables, a 100% value means a perfect match. The median differences (Δ medians) between the modeled and ERA5 are computed by the Mann-Whitney non-parametric test with a 5% significance level. The method tests the null hypothesis of two data samples belonging to continuous distributions with equal medians. Low median differences mean a better fit. The detailed methodology used to compare the four models is described in Ref. [38].

Climatic monthly changes were retrieved for the present and two future climate periods. For the baseline climate, the median year for the period comprised between 1985 and 2014 was established. The timeframes for the two future climates are 2050 (2036–2065) and 2080 (2066–2095). Each timeframe was computed by selecting the median month for each of the 12 months of the year. For example, the month of January in present-day is the median January considering all the Januarys from 1985 to 2014. The same procedure was followed for the remaining months, and this methodology was replicated for the timeframes 2050 and 2080, considering the corresponding periods. The monthly changes were determined for the four SSPs. In addition, the extreme years (warmest and coldest years) are generated to provide the bounds to the typical future EPW. These extreme years are created by

Table 3
EPW variables, morphing procedure, and variables used in EnergyPlus. Symbols: ◆ morphed variables, • calculated variables, ▽ unchanged variables, ∅ missing values, and • used variables by EnergyPlus.

EPW variable	Future Weather Generator	EnergyPlus
N6 Dry Bulb Temperature	◆	•
N7 Dew Point Temperature	◆	•
N8 Relative Humidity	◆	•
N9 Atmospheric Pressure	◆	•
N10 Extraterrestrial Horizontal Radiation	•	
N11 Extraterrestrial Direct Normal Radiation	•	
N12 Horizontal Infrared Radiation from the Sky	•	•
N13 Global Horizontal Radiation	◆	
N14 Direct Normal Radiation	•	•
N15 Diffuse Horizontal Radiation	•	•
N16 Global Horizontal Illuminance	•	
N17 Direct Normal Illuminance	•	
N18 Diffuse Horizontal Illuminance	•	
N19 Zenith Luminance	•	
N20 Wind Direction	▽	•
N21 Wind Speed	◆	•
N22 Total Sky Cover	◆	•
N23 Opaque Sky Cover	•	•
N24 Visibility	∅	
N25 Ceiling Height	∅	
N26 Present Weather Observation	▽	•
N27 Present Weather Codes	▽	•
N28 Precipitable Water	∅	
N29 Aerosol Optical Depth	∅	
N30 Snow Depth	◆	•
N31 Days Since Last Snowfall	∅	
N32 Albedo	∅	
N33 Liquid Precipitation Depth	◆	•
N34 Liquid Precipitation Quantity	▽	
Ground Temperatures	•	•
Typical/Extreme Periods	•	•

Table 4
Climate models comparison for the overlap percentage (OP) and means differences (Δ medians).

Model	Grid points	Min daily temperature		Mean daily temperature		Max daily temperature	
		Δ medians	OP	Δ medians	OP	Δ medians	OP
EC-Earth3	131,072	−0.25 K	90.57%	−0.64 K	89.39%	−0.29 K	90.32%
MPI-ESM1-2-HR	73,728	−0.22 K	87.22%	−0.75 K	88.48%	−0.83 K	87.48%
MRI-ESM2-0	51,200	−0.15 K	89.11%	−0.22 K	89.56%	−0.14 K	89.43%
NorESM2-MM	55,296	−0.55 K	85.63%	−0.52 K	88.76%	−0.47 K	86.83%

determining the median changes of the five warmest/coldest months—*i.e.*, for each month of the generated year, the median change is determined from the five warmest/coldest months of the 30 years in the timeframe, which we sorted by their average air temperature. This procedure was adopted to guarantee that monthly changes are "typical" for an extreme year. The model's grid has an atmospheric resolution of T255 (~ 80 km) and 1.0° for the ocean (ORCA1L75).

Fig. 1 depicts the procedure workflow. After reading the EPW file (step 1) and followed by an integrity check (step 2), the GCM variables are read for each timeframe and scenario (step 3). Next, the tool uses the latitude and longitude specified in the EPW file to determine the four nearest points in the GCM world grid. Then, the tool interpolates the GCM monthly changes (step 5) for all timeframes and scenarios using a bilinear interpolation method (the user can also choose the nearest point or the average of the four nearest points) to downscale the climate data to the desired location. We assume that the four nearest points define a hyperbolic paraboloid surface for each GCM variable, and the method will adjust each GCM variable to the location of the EPW on that surface.

The sixth step refers to morphing the 'independent' EPW variables. We call these variables' independent' because they do not need other EPW variables to be pre-calculated to be morphed (Table 3 lists the morphed and calculated EPW variables, and Fig. 2 depicts the dependency between those variables). The morphing procedure is based on three main statistical transformations: 'shift,' 'stretch,' and the combination of both [1]. The 'shift' ($x = x_0 + \Delta x_m$) adds the monthly projected change (Δx_m) to the present-day variable (x_0). The 'stretch' ($x = \alpha_m \cdot x_0$) scales the present-day variable (x_0) by multiplying it by the fraction of the monthly projected change (α_m). When 'shift' and 'stretch' are combined, $x = x_0 + \Delta x_m + \alpha_m \cdot (x - x_0)$, the mean and variance of the present-day variable, or just the variance, are adjusted. The EPW variable 'Dry Bulb Temperature' is 'stretch' and 'shift,' while 'Dew Point Temperature,' 'Relative Humidity,' 'Atmospheric Pressure,' 'Global Horizontal Radiation,' 'Total Sky Cover,' and 'Opaque Sky Cover' are 'shift.' Lastly, 'Wind Speed,' 'Snow Depth,' and 'Liquid Precipitation Depth' variables are 'stretch.' The complete description of the mathematical formulation can be found in the tool's documentation in Ref. [39].

Step 7 determines the 'dependent' variables from the morphed future variables in step 6. The future 'dependent' variables are calculated from psychrometric functions [40,41] and solar model equations [42–44]. In the case of the ground temperatures, the values are determined following the procedure presented in the technical manual of the CCWorldWeatherGen [45], which is, in turn, based on the EnergyPlus Weather Converter routine for ground temperature calculation [46]. Also, the Typical/Extreme Periods are calculated to determine each season's typical and extreme weeks. The typical periods are determined by finding the week with the average dry bulb temperatures nearest to the average of each four seasons. The extreme periods are the weeks with the average dry bulb temperatures nearest the maximum and minimum dry bulb temperatures of the summer and winter seasons, respectively.

In step 8, the irradiance and illuminance variables are computed. At the end of the calculations, some variables are unchanged in the generated EPW file. For example, the 'wind direction' variable values are preserved since these cannot be morphed or calculated in any other way. An alternative would be to set these values as missing; however, that would, for instance, greatly limit the EnergyPlus outside surface convection calculations when using the generated EPW files. By including wind direction, even if unchanged, we leave that choice to the user, who may opt for the adequate outside surface convection algorithm (which may or not include wind direction). As the morphing procedure does not change the weather pattern, the 'Present Weather Observation,' 'Present Weather Codes,' and 'Liquid Precipitation Quantity' variables are also unchanged. In addition, EnergyPlus only uses these to determine when it is raining at a specific time step to override the outside surface convection coefficients. Finally, the app sets the remaining variables as missing, as these are not employed in EnergyPlus (step 9). After the variables are set, their integrity and limits are checked (step 10). Afterward, the new EPW file for the currently processed timeframe and scenario is saved (step 11). The last step in this loop (12) is to save the comparison table between the original EPW and generated EPW files, the monthly changes of the GCM variables, and the

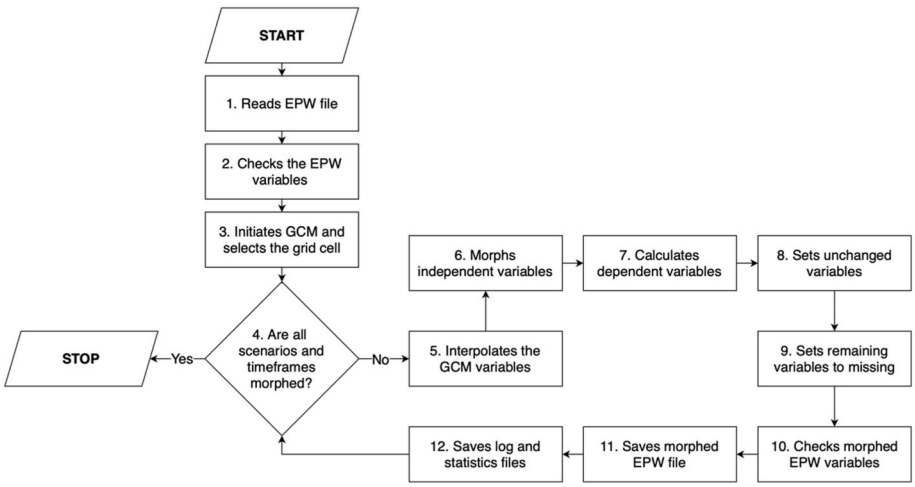

Fig. 1. The workflow for morphing the data of an EPW file.

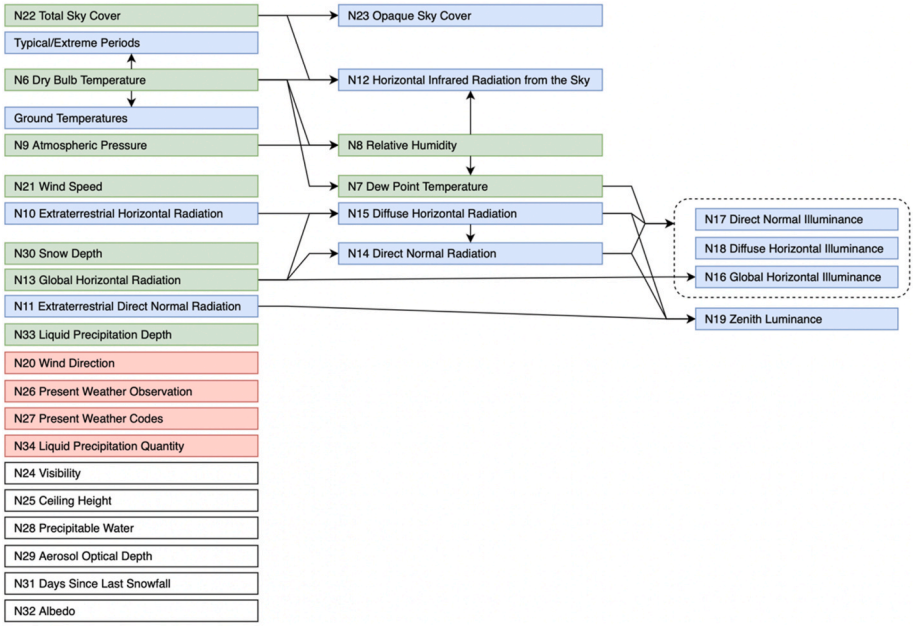

Fig. 2. Flowchart of the variables' dependencies. Green-colored boxes are morphed variables, blue-colored boxes are calculated variables, red-colored boxes are unchanged variables, and non-colored boxes are variables set to missing. (For interpretation of the references to color in this figure legend, the reader is referred to the Web version of this article.)

warnings log file. When all the timeframes and scenarios are processed, the tool stops.

We have developed the tool in Java programming language [47] to be cross-platform and called it the 'Future Weather Generator.' The tool and its source code are free to download and available under the Creative Commons Attribution 4.0 Share-Alike license [48]. It may be used as a stand-alone application when using the graphic user interface or running from the command line. Researchers can also use it as an external library in a Java project. The app is open-source software, so that the code project may be cloned, forked, or downloaded.

3. Showcase

As an example of the application of the new tool, the 'TecBIS Building E' (outside view depicted in Fig. 3), located at the Instituto Pedro Nunes (IPN) in Coimbra, Portugal, is simulated for the current and two future scenarios (2050 and 2080). The goal is to understand the variation in the building's thermal and electrical energy demand while maintaining comfort standards. The simulation model was previously validated for energy certification purposes.

The building consists of three floors. The ground floor is a garage area (floor area of 772 m^2), the first floor is occupied by meeting rooms, offices, and open office space (floor area of 688 m^2), and the second floor is another open office space (floor area of 688 m^2). Other technical, circulation, and bathroom spaces are spread across the three floors. The edifice has its main façades facing north and south, with most glazed surfaces facing north.

The building is used by different technological companies, with an occupation rate of 0.18 person per m^2 in the working zones, a lighting design level of 6.8 kW in the working areas (7.5 W m^{-2}) and 7.1 kW in the remaining ones (6.5 W m^{-2}), and an average electric equipment design level of 6.15 kW. These internal gains are all subject to specific zone occupation/operating schedules.

The Heating, Ventilating, and Air Conditioning (HVAC) for the offices, meeting rooms, and open spaces is provided by a set of fan coil (FC) units and a fresh air handling unit (FAHU) that are fed by an electric chiller/heat pump. The heating and cooling setpoints for the HVAC terminal equipment are 22 °C and 24 °C, respectively, and are scheduled

Fig. 3. IPN's 'TecBIS building E' in Coimbra, Portugal.

to operate during the working hours—8:00–19:00. In addition, two variable refrigerant flow (VRF) units are responsible for cooling two data center rooms (constant setpoint of 19 °C). All zones in contact with the exterior through doors or windows present an infiltration flow rate of 0.4 air changes per hour (ACH) when the FAHU is off. In addition, the garage is open to the outside environment, presenting a constant infiltration of 10 ACH.

The thermal capacity of the HVAC equipment is sized automatically by EnergyPlus, depending on the climatic conditions of the respective scenario. For each scenario (current, 2050, and 2080), the summer and winter design conditions for the equipment's sizing calculations correspond to the extreme summer and winter periods of the generated weather file, respectively. This choice prevents any capacity limitation that the equipment may face (not being able to satisfy the thermal needs) since the current equipment was not designed specifically for each future climate scenario. Notice also that the HVAC equipment efficiency is considered constant, independently of the climate scenario,

since it is impossible to predict the future increment in efficiency accurately. Some available projections depend on the considered scenario; however, the assessment of the future operation of the HVAC equipment is not in the scope of this work. The aim here is merely to present an idea of the variation in energy consumption that may occur given future climate changes.

The weather file for Coimbra's current conditions was obtained from the Climate.OneBuilding.Org website [35]. It was then morphed for SSP1-2.6, SSP2-4.5, SSP3-7.0, and SSP5-8.5, and the median year of 2050 and 2080 timeframes for the GCM EC-Earth3, using the 'Future Weather Generator' tool.

Subsequently, a broader assessment is presented, encompassing results from distinct cooling- and heating-dominated climates across Europe, namely, Athens, Madrid, Rome, Paris, Copenhagen, and Helsinki. For this purpose, the same building, systems, and usage were considered. Only the opaque and transparent external elements' thermal resistance values were altered to suit the respective climate, according to the current legal requirements for each country. Also, only the 2050 SSP2-4.5 case is considered due to its imminence and higher probability of occurrence. The weather files were obtained from the Climate.OneBuilding.Org website [35] and morphed for SSP2-4.5 and the median year of 2050 using the 'Future Weather Generator' tool.

4. Results and discussion

4.1. Showcase results

As a demonstration of the 'Future Weather Generator,' Table 5 presents the average annual values of selected current environment variables and the respective variation for the 2050 and 2080 timeframes (morphing output). The morphing result for Coimbra follows the global trend. There is an increase in temperatures, solar radiation, and illuminance in future scenarios, which are more acute as the scenario is more severe than the present-day climate. Moreover, the opposite tendency can be seen for the 'Relative Humidity,' 'Total Sky Cover,' and 'Liquid Precipitation Depth.'

This climate data variation directly impacts the thermal energy requirements of future buildings and, consequently, their HVAC equipment energy usage. Table 6 presents the annual heating and cooling thermal energy needs for the occupied building zones, for the current, 2050, and 2080 timeframes, by maintaining the current comfort levels. It also shows the total annual electric energy consumed by the chiller/heat pump to satisfy the thermal requirements and operation hours. The thermal and electric energy requirements of the data center rooms and their VRF units, which operate continuously, are also presented.

As expected, with the changes in solar radiation as well as air temperatures in future scenarios, heating energy requirements tend to decrease while cooling needs increase. This change in the outdoor conditions directly impacts the HVAC equipment's electric consumption and operation hours. For the worst-case scenario (SSP5-8.5), both thermal energy demand and electricity use for heating present a reduction of *circa* 60% in 2050 and 77% in 2080, compared to the current case, which translates into a 27% and 44% decrease in the heating production hours, respectively. However, the cooling thermal energy requirements and the respective electricity consumption will increase by *circa* 67% in 2050 and 121% in 2080, for which the chiller/heat pump needs to operate for 31% and 51% more hours, respectively. Consequently, given the higher energy needs for cooling than for heating, global electricity consumption will increase by 24% in 2050 and by 53% in 2080. However, this growth is limited to 14% and 15% in 2050 and 2080, respectively, for the best-case scenario (SSP1-2.6). Furthermore, if we consider the higher future electricity consumption of the VRF units, the global electric energy consumption further increases.

Keep in mind that these results were obtained considering constant efficiency values for the HVAC equipment, which may happen in a worst-case scenario, thus giving us a clearer picture of the future building performance for the most unfavorable situation. Given the constant efficiency considered for the chiller/heat pump, its efficiency would need to increase on average by a factor of 1.7 in 2050 and by 2.2 in 2080 to maintain the current electricity consumption values for cooling.

We extended the analysis to present a broader assessment of the impact of climate change, encompassing distinct cooling- and heating-dominated regions. The results are shown in Table 7. As can be seen, the rise in temperature and solar radiation is common in all locations. Regarding the HVAC, even in the locations where heating overcomes cooling (Paris, Copenhagen, and Helsinki), the tendency is for a significant heating demand decrease (at least 24%) and a very high cooling requirement increase (at least 51%; excluding the VRF equipment, for which the increase is minimal in all cases). In fact, for these locations, apart from Paris, the decrease in heating demand overcomes the cooling demand increment (absolute values). Also, notice that as opposed to the warmer locations, the total HVAC energy needs (cooling and heating) tend to remain constant or even decrease in the future in the heating-dominated climates, mainly due to the significant heating demand decrease. This trend is even more noticeable for higher latitudes (*e.g.*, Helsinki will have −11% of total electric energy consumption for HVAC in 2050 when compared to the present case).

These results exemplify the impact of climate change on the thermal energy performance of a real-case office building. Although expected, these serve mainly to test some of the tool's outputs. It is crucial to have accurate and reliable weather data to reduce the risk of underdimensioning systems, which may be modeled to match those predictions. Also, it shows the value of estimation using up-to-date future weather data morphed from the latest historical records (*i.e.*, from the 21st century).

Table 5
Average annual environmental variables for the current timeframe and their variation for the median year of 2050 and 2080 timeframes. The future timeframes generated with the Future Weather Generator tool consider four distinct SSPs.

Variable	Current	2050				2080			
		SSP1-2.6	SSP2-4.5	SSP3-7.0	SSP5-8.5	SSP1-2.6	SSP2-4.5	SSP3-7.0	SSP5-8.5
Dry Bulb Temperature [°C]	15.1	+1.7	+1.7	+2.3	+2.7	+1.9	+2.5	+3.5	+4.6
Dew Point Temperature [°C]	10.3	+1.2	+1.2	+1.4	+1.8	+1.1	+1.5	+2.0	+2.3
Relative Humidity [%]	76.5	−1.0	−1.5	−2.7	−1.7	−2.2	−2.6	−3.8	−5.6
Atmospheric Pressure [Pa]	99870.9	+19.0	+1.8	−5.3	−29.7	−21.4	+11.6	−17.0	−11.7
Horizontal Infrared Radiation from the Sky [W/m^2]	349.1	+24.6	+23.3	+25.4	+28.7	+24.2	+26.3	+30.5	+37.2
Direct Normal Radiation [W/m^2]	171.2	+17.0	+16.1	+17.0	+12.9	+18.0	+19.3	+18.5	+18.3
Diffuse Horizontal Radiation [W/m^2]	72.7	−4.1	−3.7	−4.2	−3.1	−4.7	−4.6	−4.3	−4.6
Direct Normal Illuminance [lux]	16329.5	+1722.9	+1609.7	+1724.3	+1258.9	+1862.8	+1921.9	+1808.3	+1805.4
Wind Speed [m/s]	2.27	−0.01	−0.02	−0.01	+0.02	+0.02	−0.03	−0.09	−0.01
Total Sky Cover []	6.71	0.00	−0.15	−0.31	−0.24	−0.17	−0.38	−0.62	−0.54
Opaque Sky Cover []	6.71	0.00	−0.15	−0.31	−0.24	−0.17	−0.38	−0.62	−0.54
Liquid Precipitation Depth [mm]	48.0	−0.7	−4.0	−1.9	−1.1	+2.1	−6.3	−8.3	−6.0

Table 6
Annual heating and cooling thermal and electric energy requirements and thermal energy production hours for the current timeframe and their variation for the median year 2050 and 2080 timeframes, considering the IPN's 'TecBIS Building E' case.

Variable	Current		2050							
	Total	Intensity		SSP1-2.6		SSP2-4.5		SSP3-7.0		SSP5-8.5
Total Heating Energy Needs [MJ]	46350	44.7 MJ m^{-2}	−19086	−41%	−17421	−38%	−24640	−53%	−27277	−59%
Total Heating Electric Energy [MJ]	17521	16.9 MJ m^{-2}	−7387	−42%	−6655	−38%	−9537	−54%	−10565	−60%
Heating production [h]	2609	–	−436	−17%	−409	−16%	−601	−23%	−704	−27%
Total Cooling Energy Needs [MJ	113231	109.2 MJ m^{-2}	+48303	43%	+50764	45%	+62416	55%	+75610	67%
Total Cooling Electric Energy [MJ]	34343	33.1 MJ m^{-2}	+14552	42%	+15287	45%	+18797	55%	+22777	66%
Cooling production [h]	1749	–	+376	21%	+364	21%	+475	27%	+549	31%
Total Cooling Energy Needs – VRF [MJ]	200874	12115.4 MJ m^{-2}	+4555	2%	+4627	2%	+5871	3%	+6648	3%
Total Cooling Electric Energy – VRF [MJ]	59205	3570.9 MJ m^{-2}	+1342	2%	+1364	2%	+1731	3%	+1959	3%
Variable	Current		2080							
	Total	Intensity	SSP1-2.6		SSP2-4.5		SSP3-7.0		SSP5-8.5	
Total Heating Energy Needs [MJ]	46350	44.7 MJ m^{-2}	−20078	−43%	−23952	−52%	−29021	−63%	−35635	−77%
Total Heating Electric Energy [MJ]	17521	16.9 MJ m^{-2}	−7795	−44%	−9180	−52%	−11131	−64%	−13538	−77%
Heating production [h]	2609	–	−382	−15%	−583	−22%	−911	−35%	−1138	−44%
Total Cooling Energy Needs [MJ]	113231	109.2 MJ m^{-2}	51143	45%	74020	65%	109223	96%	137052	121%
Total Cooling Electric Energy [MJ]	34343	33.1 MJ m^{-2}	15387	45%	22248	65%	32837	96%	41211	120%
Cooling production [h]	1749	–	362	21%	497	28%	668	38%	897	51%
Total Cooling Energy Needs – VRF [MJ]	200874	12115.4 MJ m^{-2}	4936	2%	6528	3%	8850	4%	11123	6%
Total Cooling Electric Energy – VRF [MJ]	59205	3570.9 MJ m^{-2}	1455	2%	1924	3%	2608	4%	3278	6%

Table 7
Average annual environmental variables for the current timeframe and their variation for the median year of 2050, and annual heating and cooling thermal and electric energy requirements and thermal energy production hours for the current timeframe and their variation for the median year 2050, in different climates.

Variable	Athens		Madrid		Rome	
	Current	2050 SSP2-4.5	Current	2050 SSP2-4.5	Current	2050 SSP2-4.5
Dry Bulb Temperature [°C]	18.4	+2.0	14.4	+2.5	16.3	+2.5
Relative Humidity [%]	61.8	−0.7	53.8	−3.7	73.3	−2.5
Horizontal Infrared Radiation from the Sky [W/m2]	353.6	+17.9	326.4	+9.7	346.5	+24.9
Direct Normal Radiation [W/m2]	227.7	+14.1	214.4	+22.7	209.8	+15.3
Diffuse Horizontal Radiation [W/m2]	69.4	−4.3	68.3	−6.8	67.3	−3.5
Total Sky Cover []	4.2	−0.3	3.7	−0.2	4.7	−0.1
Liquid Precipitation Depth [mm]	17.7	−1.3	29.7	−3.6	66.3	+0.8
Total Heating Energy Needs [MJ]	37436	−14852 (−40%)	76494	−20476 (−27%)	46201	−20266 (−44%)
Total Heating Electric Energy [MJ]	14427	−5688 (−39%)	30172	−8409 (−28%)	17818	−8164 (−46%)
Heating production [h]	2057	−427 (−21%)	2616	−316 (−12%)	2359	−459 (−19%)
Total Cooling Energy Needs [MJ	238044	+72837 (+31%)	156612	+62139 (+40%)	188576	+85136 (+45%)
Total Cooling Electric Energy [MJ]	71735	+21871 (+30%)	47230	+18536 (+39%)	56729	+25729 (+45%)
Cooling production [h]	2584	+376 (+15%)	1911	+367 (+19%)	2080	+557 (+27%)
Total Cooling Energy Needs – VRF [MJ]	210185	+4858 (+2%)	202419	+5342 (+3%)	206055	+5540 (+3%)
Total Cooling Electric Energy – VRF [MJ]	56049	+1295 (+2%)	53979	+1425 (+3%)	54948	+1477 (+3%)
Total HVAC Thermal Energy Needs [MJ]	485664	+62842 (+13%)	435525	+47005 (+11%)	440832	+70410 (+16%)
Total HVAC Electric Energy [MJ]	142211	+17478 (+12%)	131381	+11552 (+9%)	129495	+19042 (+15%)
Variable	Paris		Copenhagen		Helsinki	
	Current	2050 SSP2-4.5	Current	2050 SSP2-4.5	Current	2050 SSP2-4.5
Dry Bulb Temperature [°C]	11.8	+1.9	9.4	+2.1	7.0	+2.5
Relative Humidity [%]	73.0	+0.3	79.5	−0.5	79.7	−0.5
Horizontal Infrared Radiation from the Sky [W/m2]	326.3	+21.4	316.1	+25.0	304.5	+26.9
Direct Normal Radiation [W/m2]	97.9	+15.8	93.7	+11.3	94.9	−4.6
Diffuse Horizontal Radiation [W/m2]	75.7	−3.3	66.7	−1.3	56.4	+1.7
Total Sky Cover []	5.6	−0.1	6.2	0.0	6.3	0.0
Liquid Precipitation Depth [mm]	30.7	+0.5	39.1	+3.0	43.3	+8.0
Total Heating Energy Needs [MJ]	125108	−32298 (−26%)	175500	−44480 (−25%)	213853	−58493 (−27%)
Total Heating Electric Energy [MJ]	49748	−13162 (−26%)	70402	−18234 (−26%)	86124	−24189 (−28%)
Heating production [h]	3160	−280 (−9%)	3466	−292 (−8%)	3581	−129 (−4%)
Total Cooling Energy Needs [MJ	66816	+42142 (+63%)	49472	+32324 (+65%)	46106	23541 (+51%)
Total Cooling Electric Energy [MJ]	20279	+12742 (+63%)	15053	+9823 (+65%)	14045	7108 (+51%)
Cooling production [h]	1423	+264 (+19%)	1204	+254 (+21%)	1153	248 (+22%)
Total Cooling Energy Needs – VRF [MJ]	195841	+4242 (+2%)	192316	+4112 (+2%)	190895	4251 (+2%)
Total Cooling Electric Energy – VRF [MJ]	52224	+1131 (+2%)	51284	+1097 (+2%)	50905	1134 (+2%)
Total HVAC Thermal Energy Needs [MJ]	387765	+14086 (+4%)	417287	−8044 (−2%)	450854	−30701 (−7%)
Total HVAC Electric Energy [MJ]	122251	+711 (+1%)	136739	−7314 (−5%)	151074	−15948 (−11%)

5. Discussion

'Future Weather Generator' uses the latest and state-of-the-art GCM data—translating into higher accuracy and finer grid resolution. Using state-of-the-art climate data is fundamental, as past climate models underestimate observed global warming (CMIP5 models show the best agreement of all; however, the number of observed years is still small to draw a definitive conclusion about CMIP6 models) [49]. Fig. 4 depicts the spatial resolution of the climate models in both CCWorldWeatherGen and 'Future Weather Generator.' As we can observe, the coarse spatial resolution of CCWorldWeatherGen only has a single point over the Portuguese territory. In addition, CCWorldWeatherGen averages the four nearest points, meaning that any location within the limits of the cell defined by these four points will have the same values. In the case of the 'Future Weather Generator,' not only the spatial resolution is significantly finer, but the bilinear interpolation method also spatially downscales the climate model variables to the location of the building. Hence, combining finer spatial resolution with a better interpolation method allows us to have more precise discretization of future weather data.

In addition, 'Future Weather Generator' generates weather considering more variables than other tools, such as CCWorldWeatherGen and 'Weather Morph.' For example, it guarantees that dynamic simulation calculates the impact of rain and snow on the heat convection coefficients of the building envelope and ground reflectance by morphing 'Liquid Precipitation Depth' and 'Snow Depth,' respectively. Fig. 5 depicts examples of using weather generated by CCWorldWeatherGen and 'Future Weather Generator' from the same baseline weather and building. The top graph shows EnergyPlus does not consider the surfaces to be wet when using weather generated by CCWorldWeatherGen. The lack of rainfall occurs due to CCWorldWeatherGen setting 'Present Weather Observation' and 'Present Weather Codes' as missing; thus, EnergyPlus calculates the convection heat transfer coefficient of these elements as being dry. When rainfall is signaled, like in weather generated by the 'Future Weather Generator,' EnergyPlus overrides the calculation of the convection heat transfer coefficient of the outside

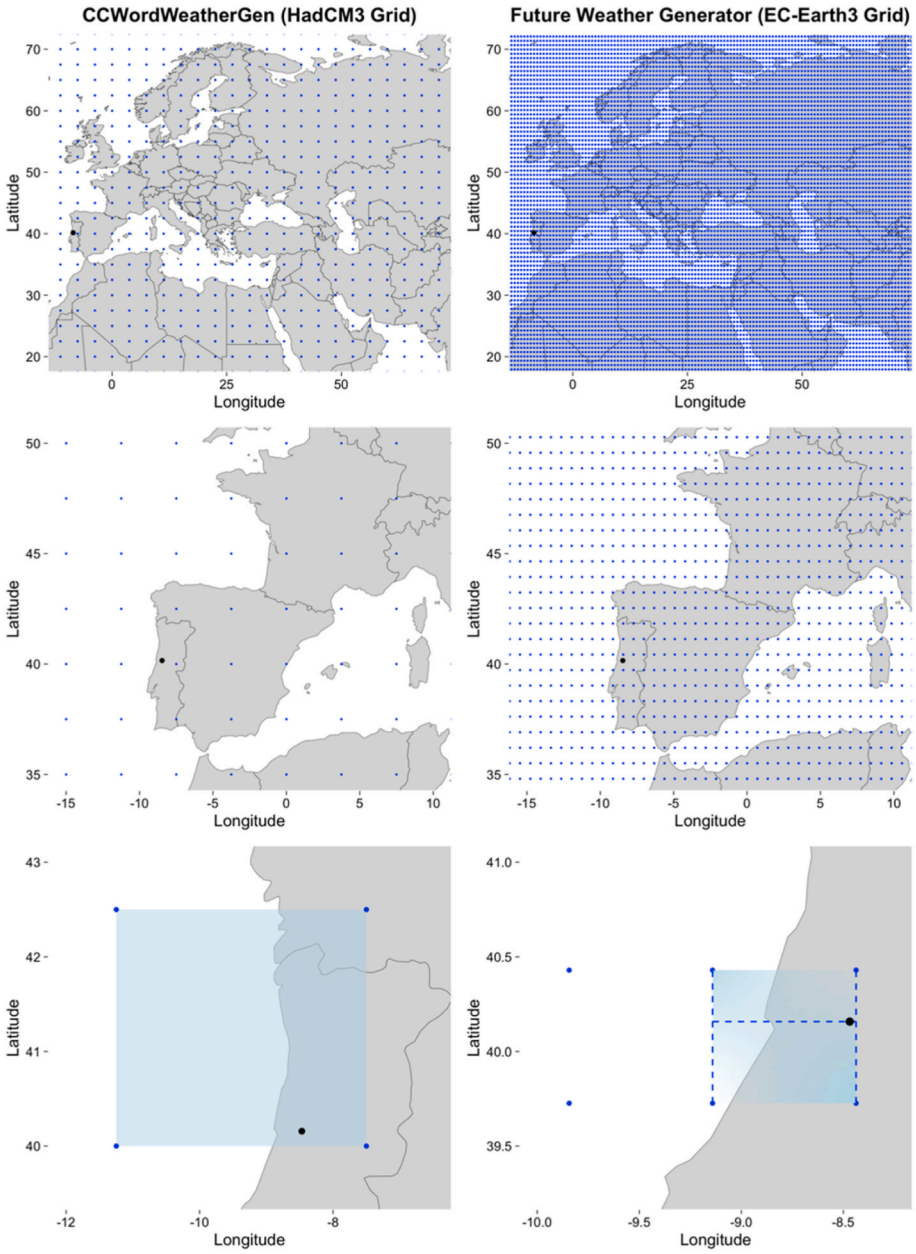

Fig. 4. Comparison of the spatial resolution between CCWorldWeatherGen and 'Future Weather Generator' climate models (HadCM3 and EC-Earth3, respectively) over Europe, North Africa, and the Middle East (top row graphs) and over the Iberian Peninsula and France (middle row graphs). The bottom row graphs depict the spatial downscale used in CCWorldWeatherGen and 'Future Weather Generator.' Blue dots are the climate model's grid points. The black dot is the location of the showcase. (For interpretation of the references to color in this figure legend, the reader is referred to the Web version of this article.)

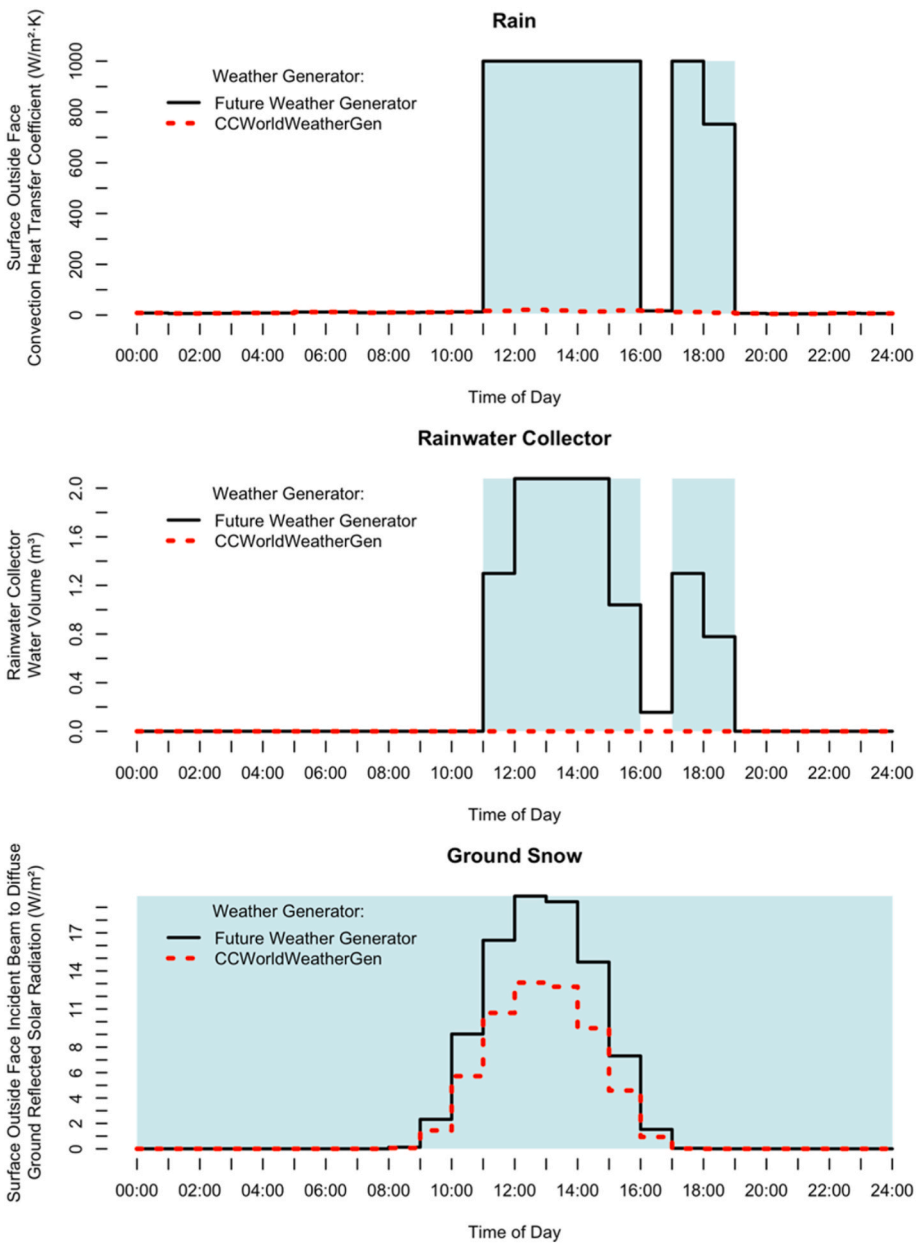

Fig. 5. CCWorldWeatherGen (dashed red line) *versus* 'Future Weather Generator' (solid black line). The blue background depicts the period when rain occurs or when snow covers the ground in the baseline weather (Coimbra and Stockholm, respectively). These examples were built solely for comparison of procedure purposes, as both tools have different baseline periods, climate change scenarios, and future timeframes. (For interpretation of the references to color in this figure legend, the reader is referred to the Web version of this article.)

surface face with a high and fixed value of 1000 W m^{-2} K^{-1}. Although this is a questionable simplification of the impact of rain events by EnergyPlus [50], it is well-known that heat transfer at exterior building surfaces is influenced by moisture fluxes [51] and should not be disregarded.

The absence of signaling occurrence of rain, combined with not morphing 'Liquid Precipitation Depth,' may also affect water systems in EnergyPlus. For example, as illustrated by the middle graph in Fig. 5, the volume of collected rainwater in a Rainwater Collector installed in a building is zero using CCWorldWeatherGen weather data. This limitation may impact the performance of other objects (*e.g.*, cooling towers) that might depend on collected rainwater.

The bottom graph in Fig. 5 compares the incident beam-to-diffuse ground-reflected solar radiation on a random exterior wall for both tools' generated weather. Since CCWorldWeatherGen sets 'Snow Depth' to missing and does not morph it, EnergyPlus will use a smaller ground reflectance value when compared with the case of existing snow. Therefore, the amount of incident diffuse ground-reflected solar radiation is significantly lower than when it is morphed with 'Future Weather Generator,' which morphs the variable 'Snow Depth.' According to Thevenard & Haddad [52], ground reflectivity may be responsible for up to 23% of sensible heating loads on a monthly basis.

The aspects mentioned above are critical in regions with frequent rain and snow. Nonetheless, their actual impact depends on the envelope's thermophysical properties, implemented systems, geometry, and weather characteristics where the building is located.

Another difference between the tools is the morphing of 'Relative Humidity' and 'Dew Point Temperature.' CCWorldWeatherGen uses monthly changes of the HadCM3 to shift present-day 'Relative Humidity.' The future 'Relative Humidity' is then used with future 'Dry Bulb Temperature,' future 'Atmospheric Pressure,' and future 'Partial Pressure of Water Vapor' to calculate the future 'Dew Point Temperature' using ASHRAE Psychometrics functions [40]. In the case of the 'Future Weather Generator,' the future 'Relative Humidity' is calculated after morphing 'Specific Humidity' with EC-Earth3 monthly changes. Because EPW data does not include 'Specific Humidity,' this present-day variable is pre-calculated using ASHRAE Psychometrics functions [40]. Similarly, future 'Dew Point Temperature' is determined with future 'Specific

Humidity,' future 'Atmospheric Pressure,' and future 'Dry Bulb Temperature' using ASHRAE Psychometrics functions [40]. This approach allows us to preserve the physical relationship between the morphed variables.

In addition, the 'Future Weather Generator' determines the typical and extreme periods from the morphed variables, which are included in the EPW file. This information may then be used to auto-size the HVAC systems in EnergyPlus (this information is also available in detail on the companion statistics file generated along with the EPW files).

The differences between 'Future Weather Generator' and CCWorldWeatherGen ('Weather Morph' follows a similar implementation) may be summarized as follows.

1. CCWorldWeatherGen seems to apply a linear transition to the GCM variables for the last and the first 24 h of each month (not applicable to the beginning of the first month and ending of the last month). However, in the 'Future Weather Generator,' the user may explicitly define the number of hours for a smooth transition between months.
2. CCWorldWeatherGen only averages the four nearest location points. However, the 'Future Weather Generator' allows the user to use the bilinear interpolation method, the nearest point, or an average of the four nearest points.
3. 'Future Weather Generator' does not use the GCM precipitation variable to morph EPW's 'Precipitable Water' because EnergyPlus does not use this variable.
4. 'Future Weather Generator' keeps both 'Present Weather Observation' and 'Present Weather Code' as in the original EPW file. These fields flag EnergyPlus to consider the building surfaces as wet when calculating the outside surface heat convection coefficients. CCWorldWeatherGen sets these fields to missing, thus considering the building's surfaces permanently dry.
5. CCWorldWeatherGen sets 'Liquid Precipitation Depth' to missing. However, this variable is used by EnergyPlus to determine the amount of water captured by a rainwater collector, for example. 'Future Weather Generator' uses the GCM precipitation variable to morph this EPW variable.
6. CCWorldWeatherGen sets 'Snow Depth' to missing. However, this variable is used by EnergyPlus to determine the ground reflectance. 'Future Weather Generator' morphs this variable.
7. CCWorldWeatherGen does not compute the Typical/Extreme Periods from the morphed EPW data. Contrasting, the 'Future Weather Generator' calculates six extreme/typical periods.

The 'Future Weather Generator' checks the integrity of each variable of the original EPW file (confirms missing values and imposes the variables' limits). However, the tool will morph the weather data even if this does not correspond to the period of historical data from the GCM model. Therefore, it is up to the user to guarantee that the procedure may be applied to a specific EPW file. Also, after the generation procedure is complete, the user should verify if the GCM monthly changes present reasonable values for the specified location, even though we impose a 'stretch' cap of five for the monthly changes of 'Wind Speed,' 'Liquid Precipitation Depth,' and 'Snow Depth.' Some unreasonable changes may occur in locations (less than 1% of the data points that correspond to extreme weather regions like deserts) that currently show a very low amount of those variables, but in the future small increases may lead to a large monthly change.

Although 'Future Weather Generator' is an important step forward in terms of spatial resolution, scenario options, and precision of future climate, compared to CCWorldWeatherGen, some may argue that the tool would benefit from using RCM data, as these models may have 2 to 10 times higher spatial resolution [53]. Furthermore, due to such resolution, RCM adds value in regions with variable orography, land-sea, and other contrasts [53]. Therefore, it would increase the accuracy and discretization of the tool even further. However, if we aim at having a stand-alone easy-to-use tool that encompasses the entire planet, it is not possible to include RCM in a manageable way. For example, the 'Future Weather Generator' currently has 1.1 GB of compressed data. If we consider a hypothetical implementation of RCM data having an 8-km resolution, the tool would be 25 times that size. Other issues would arise, such as existing RCM covering the entire planet, having compatible RCM domains, having the same baseline period, climate change scenarios, future timeframes, and needed variables for morphing—these are the reasons why WeatherShift, which uses an ensemble of RCMs, only morphs weather data in 259 cities and not for any location in the planet. In addition, as the local characteristics captured in the original weather data are preserved in morphing [2], the issue with GCM being insensitive to orography and other contrasts is minimized.

Notwithstanding and conscious of the benefits of better spatial discretization, we developed a version of the tool with the Weather Research & Forecasting model, which has a 6-km spatial resolution covering Portugal's mainland and made it available on the tool's website [47]. This implementation follows the same morphing procedure and shows how a researcher may use the tool's open-source code to implement different climate models for specific regions or research needs.

Concluding, morphing tools are the most used future weather generation approach used by researchers dedicated to assessing a building's performance [5], and CCWorldWeatherGen is the most popular among them [13]. As shown, 'Future Weather Generator' is not only a step forward in terms of state-of-the-art climate data, spatial resolution, and the number of scenarios compared to other morphing tools but also in terms of transparency and reproducibility of scientific research.

6. Conclusions

This paper describes the development of a new weather generation tool that overcomes several issues from existing morphing tools. The tool is free, cross-platform, and open-access. An application to a real case in Coimbra, morphing local weather data to match future climate scenarios, and extending it to other distinct European climates, exemplifies how a building's thermal energy behavior will change in the future, particularly the drop in heating needs and the significant increase in cooling needs. Such understanding helps researchers and professionals to study and define optimal building designs, as it depends on the local weather characteristics and patterns.

Therefore, a weather morphing tool such as the one presented in this paper is valuable. From a user's perspective, as the developed tool is open, free, and cross-platform, it is helpful for those who wish to analyze the impact of climate change. From a researcher's perspective, the tool is up to date with the latest GCM data, generates the warmest and coldest years, has a better spatial interpolation method, and has a greater number of morphed variables.

In addition, the fact that the tool's source code is open allows researchers to verify, customize, improve, and maintain the tool, which ensures the transparency needed for a scientific tool. The openness of the code also encourages the scientific community to engage in collaborative development, suggest enhancements, or point out issues that will ultimately push forward for more research and scientific discovery on the topic. For example, one potential future development might be the implementation of an ensemble of numerical models to improve accuracy and resolution.

CRediT authorship contribution statement

Eugénio Rodrigues: Writing – review & editing, Writing – original draft, Visualization, Validation, Software, Project administration, Methodology, Investigation, Funding acquisition, Data curation, Conceptualization. **Marco S. Fernandes:** Writing – review & editing, Writing – original draft, Validation, Software, Methodology, Investigation, Formal analysis, Conceptualization. **David Carvalho:** Writing – review & editing, Validation, Software, Methodology, Investigation.

Declaration of competing interest

The authors declare that they have no known competing financial interests or personal relationships that could have appeared to influence the work reported in this paper.

Data availability

The 'Future Weather Generator' source code is available at the URL: https://bitbucket.org/cling-project/futureweathergenerator. The tool itself can be downloaded at the URL: https://adai.pt/future-weather-generator/.

Acknowledgments

The presented work is framed under the *Energy for Sustainability Initiative* of the University of Coimbra (UC).

We acknowledge the World Climate Research Programme, which, through its Working Group on Coupled Modelling, coordinated and promoted CMIP6. In addition, we thank the climate modeling groups for producing and making available their model output, the Earth System Grid Federation (ESGF) for archiving the data and providing access, and the multiple funding agencies that support CMIP6 and ESGF.

The Portuguese Foundation for Science and Technology (FCT) supported this work [grant number PTDC/EME-REN/3460/2021]. In addition, FCT funds Eugénio Rodrigues, Marco S. Fernandes, and David Carvalho through researcher contracts [2021.00230.CEECIND, 2021.02975.CEECIND, and 2020.00563.CEECIND, respectively].

We are grateful to the Instituto Pedro Nunes (IPN) for allowing us to use the simulation model and the operational and technical data of one of its buildings as a case study. We also thank Gonçalo Brites for clarifications about the simulation model and Anabela Reis for proofreading this document.

References

[1] S. Belcher, J. Hacker, D. Powell, Constructing design weather data for future climates, Build. Serv. Eng. Technol. 26 (2005) 49–61, https://doi.org/10.1191/0143624405bt112oa.

[2] M. Herrera, S. Natarajan, D.A. Coley, T. Kershaw, A.P. Ramallo-González, M. Eames, D. Fosas, M. Wood, A review of current and future weather data for building simulation, Build. Serv. Eng. Technol. 38 (2017) 602–627, https://doi.org/10.1177/0143624417705937.

[3] D. Urge-Vorsatz, K. Petrichenko, M. Staniec, J. Eom, Energy use in buildings in a long-term perspective, Curr. Opin. Environ. Sustain. 5 (2013) 141–151, https://doi.org/10.1016/j.cosust.2013.05.004.

[4] C.N. Nielsen, J. Kolarik, Utilization of climate files predicting future weather in dynamic building performance simulation – a review, J. Phys. Conf. Ser. 2069 (2021), 012070, https://doi.org/10.1088/1742-6596/2069/1/012070.

[5] L.M. Campagna, F. Fiorito, On the impact of climate change on building energy consumptions: a meta-analysis, Energies 15 (2022) 354, https://doi.org/10.3390/en15010354.

[6] M. Hosseini, A. Bigtashi, B. Lee, Generating future weather files under climate change scenarios to support building energy simulation – a machine learning approach, Energy Build. 230 (2021), 110543, https://doi.org/10.1016/j.enbuild.2020.110543.

[7] M. Eames, T. Kershaw, D. Coley, A comparison of future weather created from morphed observed weather and created by a weather generator, Build. Environ. 56 (2012) 252–264, https://doi.org/10.1016/j.buildenv.2012.03.006.

[8] M.F. Jentsch, P.A.B. James, L. Bourikas, A.S. Bahaj, Transforming existing weather data for worldwide locations to enable energy and building performance simulation under future climates, Renew. Energy 55 (2013) 514–524, https://doi.org/10.1016/j.renene.2012.12.049.

[9] H. Yassaghi, N. Mostafavi, S. Hoque, Evaluation of current and future hourly weather data intended for building designs: a Philadelphia case study, Energy Build. 199 (2019) 491–511, https://doi.org/10.1016/j.enbuild.2019.07.016.

[10] A. Moazami, V.M. Nik, S. Carlucci, S. Geving, Impacts of future weather data typology on building energy performance – investigating long-term patterns of climate change and extreme weather conditions, Appl. Energy 238 (2019) 696–720, https://doi.org/10.1016/j.apenergy.2019.01.085.

[11] WeatherShift, March 30, 2022), https://www.weathershift.com/.

[12] A. Jiang, X. Liu, E. Czarnecki, C. Zhang, Hourly weather data projection due to climate change for impact assessment on building and infrastructure, Sustain. Cities Soc. 50 (2019), 101688, https://doi.org/10.1016/j.scs.2019.101688.

[13] M.P. Tootkaboni, I. Ballarini, M. Zinzi, V. Corrado, A comparative analysis of different future weather data for building energy performance simulation, Climate 9 (2021) 37, https://doi.org/10.3390/cli9020037.

[14] R. Lapisa, E. Bozonnet, P. Salagnac, M.O. Abadie, Optimized design of low-rise commercial buildings under various climates – energy performance and passive cooling strategies, Build. Environ. 132 (2018) 83–95, https://doi.org/10.1016/j.buildenv.2018.01.029.

[15] L. Cirrincione, A. Marvuglia, G. Scaccianoce, Assessing the effectiveness of green roofs in enhancing the energy and indoor comfort resilience of urban buildings to climate change: methodology proposal and application, Build. Environ. 205 (2021), 108198, https://doi.org/10.1016/j.buildenv.2021.108198.

[16] K. Bamdad, S. Matour, N. Izadyar, S. Omrani, Impact of climate change on energy saving potentials of natural ventilation and ceiling fans in mixed-mode buildings, Build. Environ. 209 (2022), 108662, https://doi.org/10.1016/j.buildenv.2021.108662.

[17] F.M. Baba, H. Ge, L.(Leon, R. Zmeureanu Wang, Do high energy-efficient buildings increase overheating risk in cold climates? Causes and mitigation measures required under recent and future climates, Build. Environ. 219 (2022), 109230, https://doi.org/10.1016/j.buildenv.2022.109230.

[18] IPCC's Data Distribution Centre, HadCM3 Climate Change Data, 2001. https://www.ipcc-data.org/sim/gcm_clim/SRES_TAR/hadcm3_download.html. (Accessed 21 August 2022).

[19] R. Dickinson, B. Brannon, Generating future weather files for resilience, Th Int. Conf. Passiv. Low Energy Archit. Cities, Build. People Towar. Regen. Environ. 36 (2016).

[20] S. Pusat, İ. Ekmekçi, M.T. Akkoyunlu, Generation of typical meteorological year for different climates of Turkey, Renew. Energy 75 (2015) 144–151, https://doi.org/10.1016/j.renene.2014.09.039.

[21] A. Jiang, X. Liu, E. Czarnecki, Weather Morph: Climate Change Weather File Generator, 2019. http://139.62.210.131/weatherGen/. (Accessed 21 August 2022).

[22] Y. Zou, K. Xiang, Q. Zhan, Z. Li, A simulation-based method to predict the life cycle energy performance of residential buildings in different climate zones of China, Build. Environ. 193 (2021), 107663, https://doi.org/10.1016/j.buildenv.2021.107663.

[23] R. Silva, S. Eggimann, L. Fierz, M. Fiorentini, K. Orehounig, L. Baldini, Opportunities for passive cooling to mitigate the impact of climate change in Switzerland, Build. Environ. 208 (2022), 108574, https://doi.org/10.1016/j.buildenv.2021.108574.

[24] K. Bamdad, S. Matour, N. Izadyar, T. Law, Introducing extended natural ventilation index for buildings under the present and future changing climates, Build. Environ. 223 (2022), 109688, https://doi.org/10.1016/j.buildenv.2022.109688.

[25] CH2018 – Climate Change Scenarios for Switzerland, 2018. www.climate-scenarios.ch. (Accessed 23 October 2022).

[26] D. Shi, Y. Gao, P. Zeng, B. Li, P. Shen, C. Zhuang, Climate adaptive optimization of green roofs and natural night ventilation for lifespan energy performance improvement in office buildings, Build. Environ. 223 (2022), 109505, https://doi.org/10.1016/j.buildenv.2022.109505.

[27] D.C. Ince, L. Hatton, J. Graham-Cumming, The case for open computer programs, Nature 482 (2012) 485–488, https://doi.org/10.1038/nature10836.

[28] A. Morin, J. Urban, P.D. Adams, I. Foster, A. Sali, D. Baker, P. Sliz, Shining light into black boxes, Science 80 (336) (2012) 159–160, https://doi.org/10.1126/science.1218263.

[29] J.M. Pearce, Economic savings for scientific free and open source technology: a review, HardwareX 8 (2020), e00139, https://doi.org/10.1016/j.ohx.2020.e00139.

[30] A. Prlić, J.B. Procter, Ten simple rules for the open development of scientific software, PLoS Comput. Biol. 8 (2012), e1002802, https://doi.org/10.1371/journal.pcbi.1002802.

[31] M. Santamouris, C. Cartalis, A. Synnefa, D. Kolokotsa, On the impact of urban heat island and global warming on the power demand and electricity consumption of buildings—a review, Energy Build. 98 (2015) 119–124, https://doi.org/10.1016/j.enbuild.2014.09.052.

[32] K. Bamdad, M.E. Cholette, S. Omrani, J. Bell, Future energy-optimised buildings — addressing the impact of climate change on buildings, Energy Build. 231 (2021), 110610, https://doi.org/10.1016/j.enbuild.2020.110610.

[33] EnergyPlus Weather File Data Dictionary, 2022. https://bigladdersoftware.com/epx/docs/22-1/auxiliary-programs/energyplus-weather-file-epw-data-dictionary.html. (Accessed 31 March 2022).

[34] EnergyPlus Weather Data, 2022. https://energyplus.net/weather. (Accessed 31 March 2022).

[35] Climate OneBuilding, Org – Repository of Free Climate Data for Building Performance Simulation, 2021. http://climate.onebuilding.org/default.html. (Accessed 27 May 2021).

[36] R. Döscher, M. Acosta, A. Alessandri, P. Anthoni, T. Arsouze, T. Bergman, R. Bernardello, S. Boussetta, L.-P. Caron, G. Carver, M. Castrillo, F. Catalano, I. Cvijanovic, P. Davini, E. Dekker, F.J. Doblas-Reyes, D. Docquier, P. Echevarria, U. Fladrich, R. Fuentes-Franco, M. Gröger, J.v. Hardenberg, J. Hieronymus, M. P. Karami, J.-P. Keskinen, T. Koenigk, R. Makkonen, F. Massonnet, M. Ménégoz, P. A. Miller, E. Moreno-Chamarro, L. Nieradzik, T. van Noije, P. Nolan, D. O'Donnell, P. Ollinaho, G. van den Oord, P. Ortega, O.T. Prims, A. Ramos, T. Reerink, C. Rousset, Y. Ruprich-Robert, P. Le Sager, T. Schmith, R. Schrödner, F. Serva, V. Sicardi, M. Sloth Madsen, B. Smith, T. Tian, E. Tourigny, P. Uotila, M. Vancoppenolle, S. Wang, D. Wårlind, U. Willén, K. Wyser, S. Yang, X. Yepes-Arbós, Q. Zhang, The EC-earth3 Earth system model for the coupled model

intercomparison project 6, Geosci. Model Dev. (GMD) 15 (2022) 2973–3020, https://doi.org/10.5194/gmd-15-2973-2022.
[37] V. Eyring, S. Bony, G.A. Meehl, C.A. Senior, B. Stevens, R.J. Stouffer, K.E. Taylor, Overview of the coupled model intercomparison project phase 6 (CMIP6) experimental design and organization, Geosci. Model Dev. (GMD) 9 (2016) 1937, https://doi.org/10.5194/gmd-9-1937-2016. –1958.
[38] D. Carvalho, A. Rocha, X. Costoya, M. DeCastro, M. Gómez-Gesteira, Wind energy resource over Europe under CMIP6 future climate projections: what changes from CMIP5 to CMIP6, Renew. Sustain. Energy Rev. 151 (2021), 111594, https://doi.org/10.1016/j.rser.2021.111594.
[39] E. Rodrigues, D. Carvalho, M.S. Fernandes, Documentation of Future Weather Generator, 2022. March 30, 2022), https://adai.pt/future-weather-generator/documentation/.
[40] 2017 ASHRAE Handbook – Fundamentals (SI Edition), ASHRAE, 2017.
[41] A.K. Singh, H. Singh, S.P. Singh, R.L. Sawhney, Numerical calculation of psychrometric properties on a calculator, Build. Environ. 37 (2002) 415–419, https://doi.org/10.1016/S0360-1323(01)00032-4.
[42] T. Kusuda, P.R. Achenbach, Earth Temperature and Thermal Diffusivity at Selected Stations in the United States, 1965.
[43] R. Perez, P. Ineichen, R. Seals, J. Michalsky, R. Stewart, Modeling daylight availability and irradiance components from direct and global irradiance, Sol. Energy 44 (1990) 271–289, https://doi.org/10.1016/0038-092X(90)90055-H.
[44] B. Ridley, J. Boland, P. Lauret, Modelling of diffuse solar fraction with multiple predictors, Renew. Energy 35 (2010) 478–483, https://doi.org/10.1016/j.renene.2009.07.018.
[45] M.F. Jentsch, Climate Change Weather File Generators: Technical Reference Manual for the CCWeatherGen and CCWorldWeatherGen Tools, University of Southampton, Southampton, 2012.
[46] L.K. Lawrie, EnergyPlus Weather Converter, Subroutine for Ground Temperature Calculation: CalcGroundTemps.F90, Fortran Code, 2003.
[47] E. Rodrigues, D. Carvalho, M.S. Fernandes, Future Weather Generator – Morphs Current Weather for Performance Simulation of Buildings in the Future, 2022. http://adai.pt/future-weather-generator/. (Accessed 9 January 2023).
[48] E. Rodrigues, D. Carvalho, M.S. Fernandes, Source Code of the Future Weather Generator, 2022. https://bitbucket.org/cling-project/futureweathergenerator.
[49] D. Carvalho, S. Rafael, A. Monteiro, V. Rodrigues, M. Lopes, A. Rocha, How well have CMIP3, CMIP5 and CMIP6 future climate projections portrayed the recently observed warming, Sci. Rep. 12 (2022), 11983, https://doi.org/10.1038/s41598-022-16264-6.
[50] M. Mirsadeghi, D. Cóstola, B. Blocken, J.L.M. Hensen, Review of external convective heat transfer coefficient models in building energy simulation programs: implementation and uncertainty, Appl. Therm. Eng. 56 (2013) 134–151, https://doi.org/10.1016/j.applthermaleng.2013.03.003.
[51] B. Blocken, J. Carmeliet, High-resolution wind-driven rain measurements on a low-rise building - experimental data for model development and model validation, J. Wind Eng. Ind. Aerod. 93 (2005) 905–928, https://doi.org/10.1016/j.jweia.2005.09.004.
[52] D. Thevenard, K. Haddad, Ground reflectivity in the context of building energy simulation, Energy Build. 38 (2006) 972–980, https://doi.org/10.1016/j.enbuild.2005.11.007.
[53] M. Rummukainen, Added value in regional climate modeling, WIREs Clim. Chang. 7 (2016) 145–159, https://doi.org/10.1002/wcc.378.